Epitaxially grown single grain boundaries in chalcopyrites

2007 J. Phys.: Condens. Matter 19 016004

(http://iopscience.iop.org/0953-8984/19/1/016004)

INSTITUTE OF PHYSICS PUBLISHING JOURNAL OF PHYSICS: CONDENSED MATTER

J. Phys.: Condens. Matter **19** (2007) 016004 (7pp) doi:10.1088/0953-8984/19/1/016004

Epitaxially grown single grain boundaries in chalcopyrites

Susanne Siebentritt[1,2], Tobias Eisenbarth[1], Angus Rockett[3], Jürgen Albert[1], Peter Schubert-Bischoff[1] and Martha Ch Lux-Steiner[1,2]

[1] Hahn-Meitner-Institut, Glienicker Strasse 100, 14109 Berlin, Germany
[2] Freie Universität Berlin, FB Physik, Arnimallee 14, 14195 Berlin, Germany
[3] Department of Materials Science and Engineering, University of Illinois, Urbana, IL 61801, USA

Received 21 June 2006, in final form 9 November 2006
Published 7 December 2006
Online at stacks.iop.org/JPhysCM/19/016004

Abstract

To allow a specific investigation of grain boundaries with a given orientation we have grown epitaxial grain boundaries of $CuGaSe_2$ by metal organic vapour phase epitaxy (MOVPE). The epitaxy on either side of the grain boundary and the $\Sigma 3$ character of the grain boundary are shown by electron back-scattering diffraction (EBSD) scans. Scanning electron microscopy (SEM) micrographs show a dense grain boundary. Transmission electron microscopy (TEM) micrographs prove that the grain boundary in the film is the direct continuation of the grain boundary in the substrate. High-resolution TEM (HRTEM) shows that the grain boundary in the film is a twin as well, and thus a $\Sigma 3$ boundary. This also justifies the use of a classification scheme that is derived for the cubic system for the tetragonal chalcopyrites. Thus by using a $\Sigma 3$ grain boundary in the cubic GaAs substrate as a template, a $\Sigma 3$ grain boundary is obtained in the tetragonal $CuGaSe_2$ film.

(Some figures in this article are in colour only in the electronic version)

1. Grain boundaries in chalcopyrites

Grain boundaries in chalcopyrites are of technological importance because the best thin-film photovoltaic modules are made with polycrystalline chalcopyrite absorbers. Nevertheless their electronic structure is not clear and is a matter of dispute [1–6]. Grain boundaries have been experimentally investigated by Hall measurements [1], Kelvin probe force microscopy (KPFM) [7, 5, 8], and transmission electron microscopy (TEM) [9, 6]. Hall measurements probe the ensemble of grain boundaries with a preference for those with low barriers. KPFM and TEM measurements allow the investigation of individual grain boundaries.

By Hall and KPFM measurements of polycrystalline $CuGaSe_2$ films an electrostatic barrier at the grain boundaries was found and was attributed to charged defects at the grain boundary [1, 2, 7]. Defects can be suspected to be formed by strained or broken bonds, as well

as native defects or impurities. Whether the grain boundaries accumulate impurities or not is also still a matter of dispute [10, 11]. Also voids have been found at grain boundaries [11]. The accumulation of native defects at grain boundaries will also influence their composition. This might have dramatic influence on the electronic structure of the grain boundaries [3, 12] and cause a neutral barrier at the grain boundary.

The grain size in these polycrystalline materials is no larger than 0.5 to 1 μm. When investigating these grain boundaries it is not always possible to clearly distinguish bulk and grain boundary effects. Additionally, the grain boundaries are often rounded and not vertical to the surface, and this will mix the effects of bulk and grain boundary for any surface method. Although in general the films show a texture, the orientation of the grain boundaries cannot be controlled. Therefore it is desirable to investigate single grain boundaries with a defined orientation.

In this contribution we report on the epitaxial growth of single grain boundaries in $CuGaSe_2$ and their structural properties.

2. Classification of grain boundaries

It has been found previously [6] that the electrical activity of grain boundaries in chalcopyrites, i.e. their defect concentration, depends on the texture of the film: the usual $\{112\}_{tet}$ texture shows reduced luminescence yield and negative band bending at the grain boundaries, while films with a predominantly $\{220\}/\{204\}_{tet}$ texture show no reduction in luminescence yield and a small positive band bending at the grain boundaries[4]. This indicates that the grain boundaries in $\{112\}_{tet}$ textured films contain more defects than those in $\{220\}/\{204\}_{tet}$ textured films. Therefore a classification is needed for the different types of grain boundary.

In general, grain boundaries can be characterized by their coincidence site lattice, CSL, i.e. the lattice of sites where the lattices of the two grains coincide (see e.g. [13]). A classification of grain boundaries is given by the Σ-value which relates the unit cell volume of the CSL to the one of the bulk lattice. Low Σ-values indicate a strong congruence between the lattices of the two grains along the grain boundary; therefore, in general, grain boundaries with low Σ-values contain fewer defects and are therefore lower in energy.

A generating function of the CSL for the cubic system has been derived in [14]. Since the tetragonal distortion of chalcopyrites is small and since the CSL concerns only the two-dimensional plane of the grain boundary, we assume the generating function for the cubic system as an approximation for the chalcopyrite system.

The generating function can be traced back to a rotation which transforms the lattice on one side of the grain boundary into the lattice on the other side. The rotation is around an axis within the grain boundary. As a simplification we assume that all grains are oriented according to the texture and that all grain boundaries are vertical. Then the common axis within the grain boundaries in a $\{112\}_{tet}$ textured film is the $[221]_{tet}$, i.e. the $\langle 111\rangle_{cub}$ axis, while in a $\{220\}/\{204\}_{tet}$ textured film the common axis is the $\langle 110\rangle_{cub}$. Applying the generating function of [14], the grain boundaries in a $\{112\}_{tet}$ textured film show a Σ-value of 7, and the grain boundaries in a $\{220\}/\{204\}_{tet}$ textured film show a Σ-value of 3. Since lower Σ-values are in general associated with lower defect densities, this explains the lower electrical activity of $\{220\}/\{204\}_{tet}$ textured films. This in turn might be the reason for the better efficiencies obtained in solar cells using absorbers with $\{220\}/\{204\}_{tet}$ texture.

[4] By the subscript 'tet' we denote directions and planes in the tetragonal system and by 'cub' the same in the cubic system.

3. Experimental methods

Semi-insulating wafers of GaAs containing one grain boundary were obtained commercially. Onto these wafers a $CuGaSe_2$ film was grown epitaxially by metal organic vapour phase epitaxy (MOVPE) in an Aixtron 200SC horizontal quartz reactor at a growth temperature of 570 °C, a pressure of 50 mbar, and a total flow of 5 l min^{-1}. The precursors were cyclopentadienyl Cu triethyl phosphine, triethyl Ga and ditertiarybutyl Se. The details of the growth process are described elsewhere [15, 16]. This method of growing grain boundaries has been applied to other semiconductors before; see e.g. [17]. The mismatch between $CuGaSe_2$ and GaAs is 0.7%. Since our films are thicker than the critical thickness and since there are Kirkendall voids at the interface between $CuGaSe_2$ and GaAs, we can assume that there is no significant stress in the films that would influence the structure of the grain boundaries.

The films were grown under Cu excess, leading to copper selenide crystallites at the surface. The films were etched in KCN to remove the copper selenides before the electrical measurements. The structure of the wafer and the film was investigated by scanning electron microscopy (SEM), electron back-scattering diffraction (EBSD) and transmission electron microscopy (TEM). SEM was performed in a LEO 1530 (GEMINI) microscope with a field emission cathode, using a secondary electron detector. EBSD was done using a detector from HKL, and TEM was done in a CM30 from Phillips with 300 kV acceleration voltage.

4. Epitaxially grown grain boundaries

The surface orientation of the wafers is (001) on one side of the grain boundary and (221) on the other side. Taking into account that the cleavage planes of GaAs are the {110} planes it can be concluded from the cleavage angles that the grain boundary is along the $[1\bar{1}0]$ direction at the surface. Thus the common axis is a ⟨110⟩ axis. The Σ-value corresponding to ⟨110⟩ axes is Σ3, as discussed above. In this case the grain boundary is a first-order twin. The orientation of the two grains and the classification of the grain boundary was confirmed by EBSD and TEM investigations (figures 1(a) and 2(a)–figure 2(b) is discussed below in the context of the nanostructure of the grain boundary in $CuGaSe_2$). The EBSD pattern shows the surface orientations as (100) and (221), and the analysis of the grain boundary yields a Σ-value of 3. The TEM micrograph shows the twin character of the grain boundary with a mirror plane along the boundary.

Onto these wafers $CuGaSe_2$ films were grown by MOVPE. The film grew epitaxially on both sides of the wafer, maintaining the respective orientation, as can be seen from figure 1(b). The EBSD pattern was analysed with respect to the cubic system. The polar plot shows the same orientations of the film as the substrate. There are more misaligned areas detected in the EBSD of the film than of the wafer. This can be attributed to the presence of Cu selenide crystallites on the surface which are not completely removed by the KCN etch. The morphology of the film was investigated by SEM (figure 3). The overview micrograph shows the surface of the film across the grain boundary. The surface on the left-hand side is smooth with Cu selenide crystallites and trenches along the [110] direction of the substrate, typical for the $\{001\}_{tet}$ surfaces of chalcopyrites [18]. The right-hand side shows a strong faceting of the surface which can be traced to the stability of the $\{112\}_{tet}$ surfaces [19, 20], which leads to a break-up of the $\{221\}_{cub}$ surfaces into $\{112\}_{tet}$ facets. This is supported by the angle between the surface and the facets.

The surface micrograph shows a peculiar behaviour of the distribution of Cu selenide crystals. More than 10 μm away from the grain boundary the distribution of crystallites on

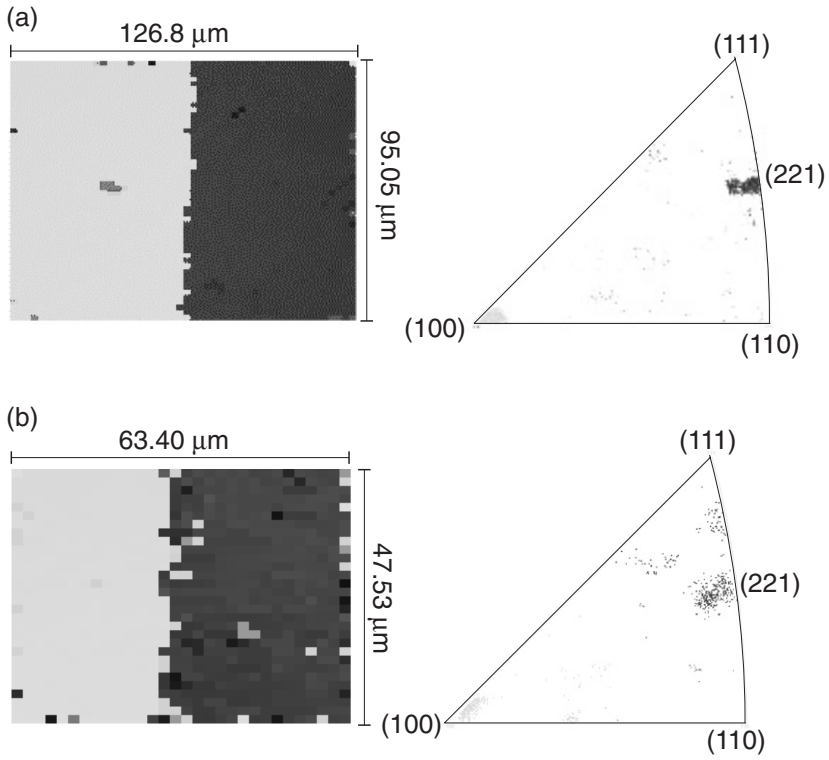

Figure 1. EBSD together with the orientation polar plots of the GaAs wafer (a) and the $CuGaSe_2$ film grown on the wafer (b). The indexing of the film was done in an approximate way with reference to the cubic system. The deviations from the main orientations can be attributed to surface defects. The EBSD of the film was taken after KCN etching, but still some Cu selenide crystals remain.

both sides is approximately equal, with a trend to larger crystallites on the $(001)_{cub}$ surface. This is attributed to the morphology: the rough surface on the $(221)_{cub}$ side allows more Cu selenide to be hidden within the surface structures. Within 10 μm of the grain boundary there are almost no crystallites on the $(001)_{cub}$ side but an accumulation of crystallites on the $(221)_{cub}$ side. Although a direct influence of the grain boundary cannot be completely excluded, this allows conclusions on the diffusion behaviour of the Cu selenide species on the surface during growth: the diffusion of the Cu selenides on the rough $(222)_{cub}$ surface is much slower than on the $(001)_{cub}$ surface. This leads to a lack of material supply from the other side of the grain boundary on the (001) surface and thus to a depletion of crystallites, and vice versa. A faster diffusion of Cu selenide species on the much smoother $(001)_{cub}$ side appears not unreasonable. Thus the accumulation of Cu selenide crystallites on the $(221)_{cub}$ side close to the grain boundary is attributed to the different diffusion behaviour of Cu selenides on the two surfaces not to a enhanced diffusion of Cu selenides towards the grain boundary.

Figure 3(b) shows a detailed micrograph of the cross section of the grain boundary in the film. The smooth $(001)_{cub}$ surface with its trenches is again seen on the left-hand side and the faceting of the $(221)_{cub}$ surface on the right-hand side. The cross section shows no clear indication of where the actual grain boundary is situated. This indicates that the grain boundary is in fact grown densely in the film without voids. Grain boundaries of this type are

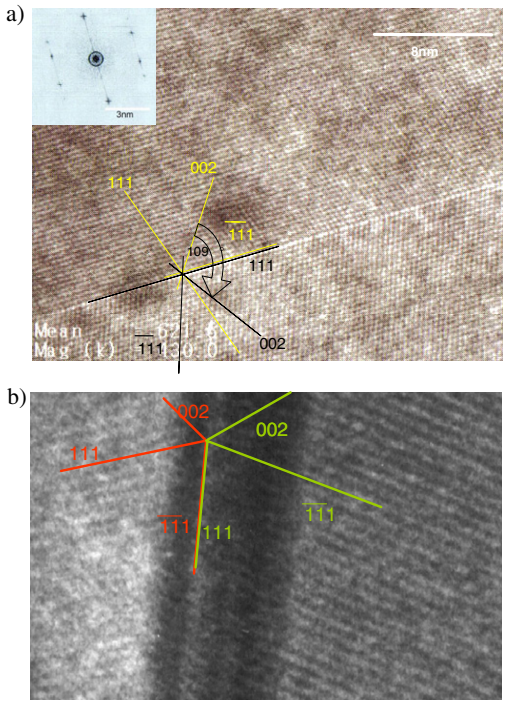

Figure 2. High-resolution TEM images of the grain boundary in the GaAs wafer (a) and the $CuGaSe_2$ film (b) together with the crystallographic orientations referenced to the cubic system. (a) shows also the diffraction pattern along the $[1\bar{1}0]$ zone axis.

only possible when grown under Cu excess. In Ga-rich or near-stoichiometric films epitaxial growth is still evident on either side of the grain boundary but the grains do not coalesce. There remains a gap of several 10 nm between the two grains.

A better resolution of the morphology of the grain boundary is obtained from TEM (figure 4). The grain boundary continues straight from the wafer into the film. At the $GaAs/CuGaSe_2$ interface Kirkendall voids are visible. These are attributed to loss of Ga from the wafer and to diffusion of vacancies, and are usually observed at the epitaxial interface between GaAs and chalcopyrites [21, 22]. The Kirkendall voids are larger in the vicinity of the grain boundary, which can be attributed to increased strain and thus accumulation of vacancies in this area.

A high-resolution micrograph of the grain boundary in the film is given in figure 2(b). The twin character of the grain boundary is evident from the mirror plane. It should be noted, though, that the twin is more defective in the film than in the wafer, as is evident from the darkened area around the grain boundary. Other TEM micrographs show kinks in the grain boundary, which were never observed for the grain boundaries in the GaAs wafer. This could imply that there is more strain in the grain boundary in the $CuGaSe_2$ film than in those in the wafer.

Thus it can be concluded that by using a $\Sigma 3$ grain boundary in the cubic substrate as a template a $\Sigma 3$ grain boundary is obtained in the tetragonal $CuGaSe_2$ film. The electrical characterization of the grain boundary in $CuGaSe_2$ is presented in a forthcoming paper [12].

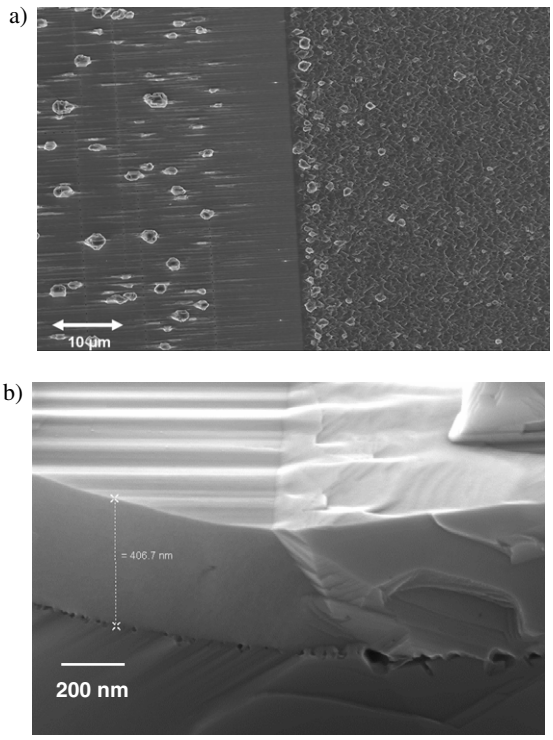

Figure 3. SEM micrograph of the grain boundary in the epitaxial $CuGaSe_2$ film. The (001) oriented part is on the left-hand side. (a) Overview of the surface. (b) Enlargement of the cross section. Both micrographs were recorded without KCN etching.

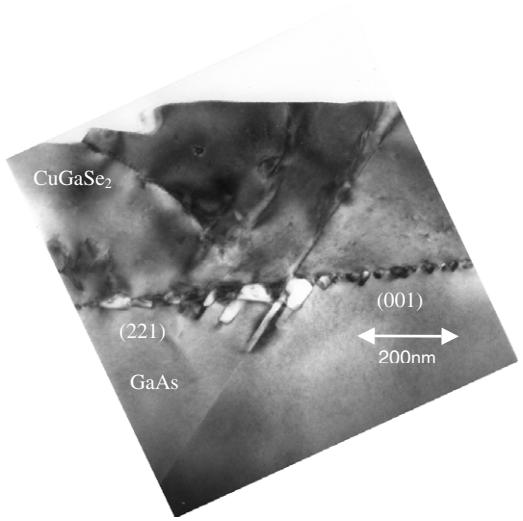

Figure 4. Large-scale TEM micrograph of the grain boundary in the wafer and the film.

5. Summary and conclusions

Applying the CSL classification scheme for grain boundaries to polycrystalline chalcopyrite films, it can be shown that in films with $\{112\}_{tet}$ texture mostly $\Sigma 7$ grain boundaries can be

expected, while in a film with $\{220\}/\{204\}_{tet}$ texture mostly $\Sigma 3$ grain boundaries are expected. Since $\Sigma 3$ grain boundaries contain fewer defects than $\Sigma 7$ grain boundaries, this explains the lower electrical activity of grain boundaries in films with $\{220\}/\{204\}_{tet}$ texture.

To allow a specific investigation of grain boundaries with a given orientation we have grown epitaxial grain boundaries. The epitaxy on either side of the grain boundary and the $\Sigma 3$ character of the grain boundary is evident from EBSD scans. SEM micrographs show a dense grain boundary. TEM micrographs prove that the grain boundary in the film is the direct continuation of the grain boundary in the substrate. HRTEM shows that the grain boundary in the film is a twin as well, and thus a $\Sigma 3$ boundary. Thus by using a $\Sigma 3$ grain boundary in the cubic GaAs substrate as a template, a $\Sigma 3$ grain boundary is obtained in the tetragonal $CuGaSe_2$ film. The observation that the grain boundary in the tetragonal film adopts the structure and the CSL from the cubic substrate justifies the use of the cubic generation function for the tetragonal structure.

Acknowledgments

We are grateful to C Kelch for the KCN etching, to I Sieber for the EBSD scans and the German Research Foundation (DFG) and the German Research Ministry (BMBF) for funding, as well as NSF for the funding through award number 0602938 (to AR).

References

[1] Schuler S, Nishiwaki S, Beckmann J, Rega N, Brehme S, Siebentritt S and Lux-Steiner M C 2002 *29th IEEE Photovoltaic Specialist Conf.* (New Orleans: IEEE) pp 504–8
[2] Siebentritt S and Schuler S 2003 *J. Phys. Chem. Solids* **64** 1621–6
[3] Persson C and Zunger A 2003 *Phys. Rev. Lett.* **91** 266401
[4] Persson C and Zunger A 2005 *Appl. Phys. Lett.* **87** 211904
[5] Fuertes Marrón D, Sadewasser S, Meeder A, Glatzel T and Lux-Steiner M C 2005 *Phys. Rev.* B **71** 033306
[6] Hanna G, Glatzel T, Sadewasser S, Ott N, Strunk H P, Rau U and Werner J H 2006 *Appl. Phys.* A **82** 1–7
[7] Sadewasser S, Glatzel T, Schuler S, Nishiwaki S, Kaigawa R and Lux-Steiner M C 2003 *Thin Solid Films* **431/432** 257
[8] Jiang C-S, Noufi R, AbuShama J A, Ramanathan K, Moutinho H R, Pankow J and Al-Jassim M M 2004 *Appl. Phys. Lett.* **84** 3477–9
[9] Ott N, Hanna G, Rau U, Werner J and Strunk H P 2004 *J. Phys.: Condens. Matter* **16** S85–9
[10] Niles D W, Al-Jassim M and Ramanathan K 1999 *J. Vac. Sci. Technol.* A **17** 291–6
[11] Lei C H, Li C-M, Rockett A, Robertson I M and Shafarman W N 2005 *Mater. Res. Soc. Symp. Proc.* **865** 93–103
[12] Siebentritt S, Sadewasser S, Wimmer M, Leendertz C, Eisenbarth T and Lux-Steiner M C 2006 *Phys. Rev. Lett.* **97** 146601
[13] Fionova L K and Artemyev A V 1993 *Grain Boundaries in Metals and Semiconductors* (Les Ulis: les editions de physique)
[14] Grimmer H 1984 *Acta Crystallogr.* A **40** 108–12
[15] Bauknecht A, Siebentritt S, Albert J and Lux-Steiner M C 2001 *J. Appl. Phys.* **89** 4391–400
[16] Artaud-Gillet M C, Duchemin S, Odedra R, Orsal G, Rega N, Rushworth S and Siebentritt S 2003 *J. Cryst. Growth* **248** 163–8
[17] Cho N-H, Carter C B, Elgat Z and Wagner D K 1986 *Appl. Phys. Lett.* **49** 29–31
[18] Siebentritt S, Papathanasiou N, Albert J and Lux-Steiner M C 2006 *Appl. Phys. Lett.* **88** 151919
[19] Jaffe J E and Zunger A 2003 *J. Phys. Chem. Solids* **64** 1547–52
[20] Zhang S B and Wei S-H 2002 *Phys. Rev.* B **65** 081402
[21] Rega N, Siebentritt S, Albert J and Lux-Steiner M C 2003 *Mater. Res. Soc. Symp. Proc.* **763** 183–8
[22] Yang L C, Chou L J, Agarwal A and Rockett A 1991 *22nd IEEE Photovoltaic Specialists Conf.* (Piscataway, NJ: IEEE) p 1185